Spin dynamics of rare-earth ions in phosphate laser glasses

I. P. Goudemond, J. M. Keartland, and M. J. R. Hoch
Department of Physics, University of the Witwatersrand, P.O. WITS 2050, Johannesburg, South Africa

G. A. Saunders
School of Physics, University of Bath, Claverton Down, Bath BA2 7AY, United Kingdom
(Received 24 August 1999; published 5 January 2001)

The spin dynamics of rare-earth ions (Er, Nd, Sm, and Gd) in heavily doped phosphate glasses have been investigated using ^{31}P NMR. A model involving inhomogeneous broadening of the NMR resonance lines, with distinct sample regions corresponding to the presence or absence of nuclear spin diffusion, has been used in extracting the electron-spin-correlation times from the NMR measurements. Correlation times in the range 10^{-2}–10^{-12} s have been obtained for temperatures between 4 and 100 K. No evidence of spin-spin coupling between the ions has been found and spin relaxation occurs via phonon processes, including the Orbach process. The importance of such processes in doped glasses is firmly established in this work. The rare-earth ions experience crystal-field effects produced by the close-to-octahedral symmetry of the local environment.

DOI: 10.1103/PhysRevB.63.054413 PACS number(s): 75.50.Kj, 76.30.Kg, 76.60.−k

I. INTRODUCTION

Magnetic and magneto-optic phenomena, of interest for optoelectronic applications, have been found in the rare-earth metaphosphate glasses (REMG) with compositions in the vicinity $(R_2O_3)_{0.25}(P_2O_5)_{0.75}$, where R is a rare-earth (RE) element. For example, these paramagnetic materials exhibit the largest known magnetic contributions to the low-temperature specific heats in oxide glasses.[1] X-ray diffraction and extended x-ray-absorption fine-structures (EXAFS) studies[2–4] have shown that the structure of REMG comprises a three-dimensional 3D network of corner-linked PO_4 tetrahedra, with the RE ions, which in several instances are known to be trivalent R^{3+}, occupying sites within the PO_4 skeleton.

Paramagnetic relaxation processes in RE-doped glasses are of interest for a number of reasons. In crystalline systems crystal fields and lattice dynamics are understood. Their roles in the various relaxation processes which occur are well established. In amorphous materials, such as the present phosphate glasses, the RE ions do not occupy sites with octahedral symmetry, although the symmetry appears to be close to this. A distribution of crystal-field interactions results in a distribution of crystal-field splittings in the ionic energy levels. If the distribution is broad, the RE ion relaxation should reflect this. Furthermore, high-frequency vibrational modes in amorphous materials are of considerable interest, and theoretical work has, for example, provided evidence for fractons. While paramagnetic relaxation does not give direct information on such modes, a comparison of the behavior in the REMG systems with that found in crystalline materials may provide indirect evidence for the importance of non-Debye behavior.

In the REMG system the paramagnetic ion relaxation times are typically extremely short (10^{-9}–10^{-12} s) except at temperatures in the liquid-helium range. Broad electron paramagnetic resonance (EPR) lines are observed with spectral diffusion preventing the measurement of paramagnetic relaxation times directly using pulsed or continuous wave EPR methods.[5]

In recent work[6] we have shown that it is possible to study the spin dynamics of RE ions in metaphosphate glasses using ^{31}P NMR as a probe. The present investigation has applied the NMR method to a number of REMG systems containing Er, Nd, Sm, and Gd ions. For some of these systems, La or Y ions have been used as a buffer in order to lower the concentration of magnetic ions while preserving the metaphosphate glass structure. Information on the dynamics of the rare-earth ions has been obtained using the model developed previously.[6]

II. MODELS AND THEORETICAL EXPRESSIONS

The structural units of the metaphosphate glasses are PO_4 tetrahedra which are linked together into chains with cross-linkage and branching of chains. RE ions occupy sites in the glassy structure such that their nearest neighbors are oxygen atoms and the structure is independent of the particular RE modifier which is present. Bowron *et al.*[2] have used EXAFS to determine the average coordination numbers for first shell oxygen atoms around a RE ion and suggest that the ions occupy a mixture of sites with pseudo-octahedral and body-centered-cubic symmetry. Octahedral sites appear to predominate and exhibit slight distortions due to the glassy structure of the host. EPR measurements[5] show that there is a large distribution of g values in these systems giving rise to broad rather featureless absorption spectra.

Spin-lattice relaxation times τ_e of the RE ions cannot be measured directly using EPR methods for reasons mentioned in Sec. I. τ_e may however be obtained from ^{31}P NMR. The nuclear spin-lattice relaxation time T_1 is measured, and τ_e is extracted using a model presented recently.[6] A brief discussion of this model follows in the interests of completeness.

While the ^{31}P spins in a phosphate glass are not arranged in a regular periodic lattice, they are sufficiently close to each other that spin diffusion, mediated by the nuclear dipole-dipole interactions, can occur. The local magnetic

field B_{loc} produced by a paramagnetic ion will produce shifts in the nuclear resonance frequencies which may inhibit spin diffusion. Furthermore, the shifts in resonance frequencies for nuclei close to an ion may result in their contribution to the NMR signal becoming unobservably weak. By introducing a mean spacing, a_0, between the nuclear spins, the radius b_0 of the diffusion barrier, inside which spin diffusion does not operate,[7] is obtained from the condition

$$a_0\left(\frac{dB_{loc}}{dr}\right)_{r=b_0}=\Delta\omega, \tag{1}$$

where $\Delta\omega$ is the natural nuclear linewidth and r is the distance measured from the ion. Using the dipolar field expression in terms of r gives

$$b_0=\left(\frac{\Delta\omega}{3a_0S}\right)^{-1/4} \tag{2}$$

for $\tau_e \gg T_2$, where τ_e is the electron correlation time and T_2 is the nuclear spin-spin relaxation time. For $\tau_e \ll T_2$ we obtain

$$b_0=\left(\frac{k_BT\Delta\omega}{3a_0\gamma_I\gamma_S^2\hbar^2S^2B}\right)^{-1/4}, \tag{3}$$

where T is the absolute temperature and B is the applied magnetic field.

It is clear from Eq. (3) that b_0 will increase as T is decreased reaching the limiting value given by Eq. (2) at sufficiently low T. Because the ^{31}P nuclei are fixed in the glass structure we do not expect any temperature dependence of the nuclear spin-diffusion coefficient D.

The ^{31}P line-shape second moment $\langle M_2\rangle$ due to nuclear dipole-dipole interactions has been estimated using available structural information. From crude calculations based on the mean spin density we obtain $\Delta\omega\simeq\sqrt{\langle M_2\rangle}=7\times10^3$ s^{-1}, which gives $T_2\simeq\Delta\omega^{-1}=140$ μs, and $D\simeq a_0^2(\sqrt{\langle M_2\rangle}/30)\sim10^{-13}$ cm^2 s^{-1}, with a fairly large uncertainty.

Nuclear spins inside the diffusion barrier contribute to the nuclear signal provided their resonance frequencies are not shifted so much that their contributions to the measured signal are unobservably weak or their frequencies lie outside the bandwidth of the spectrometer. An exclusion barrier of radius ρ_c may be defined as the radius inside which nuclei are excluded from the signal. ρ_c will have a similar temperature dependence to that of b_0 and may be written as $\rho_c\simeq b_0/k$ where k is a numerical factor larger than 1. Using $B_{loc}\sim\mu_e/r^3$, we estimate $k\simeq2.5\pm0.5$. Nuclear spins at a distance $\rho_c<r<b_0$ give rise to an inhomogeneously broadened contribution to the NMR line shape. At low temperatures b_0 and ρ_c may become sufficiently large that they overlap with the corresponding barriers associated with neighboring spins. For samples with a high concentration of paramagnetic ions, such as the present paramagnetic glasses, a significant or complete loss of nuclear signal may be expected at low temperatures. This is substantiated using numerical estimates for the distances $\langle r_{ss}\rangle$ and ρ_c, where $\langle r_{ss}\rangle$ is the mean spacing between paramagnetic ions.

The theory of nuclear spin-lattice relaxation (NSLR) due to localized, isolated paramagnetic centers in magnetically dilute crystals[7–13] has been extended to account for magnetically concentrated systems.[6] In such systems, nuclear spin diffusion may be inoperative in appreciable fractions of sample volume, and nuclei may relax to multiple paramagnetic sites. The relaxation curves have a stretched exponential or Kohlrausch form and the shape of these curves has been discussed using the theoretical expressions derived for these systems.[6]

The average nuclear relaxation rates for diffusive regions were extracted from the magnetization recovery data as a function of time τ using[6]

$$\frac{M(\tau)}{M_0}=1-2\nu\left[f\exp\left(\frac{-\tau}{T_1}\right)+(1-f)\exp\left(-\sqrt{\frac{\tau}{\lambda T_1}}\right)\right], \tag{4}$$

where ν is a scaling factor, introduced because the degree of nuclear saturation is not known precisely, and f is the diffusive fraction of nuclei. The first and second terms describe NSLR in diffusive and nondiffusive regions, respectively. The relaxation rate for nondiffusive regions has been expressed in the form[6] $T_1'=\lambda T_1$ for convenience, where λ is the ratio of the average relaxation rates for nuclei in diffusive and nondiffusive regions.

The relaxation rate for nuclei in regions where spin diffusion maintains a spin temperature is given by[6]

$$\frac{1}{T_1}=\frac{4\pi}{3}\frac{n_sC}{b^3}, \tag{5}$$

where n_s is the concentration of paramagnetic ions and b is the larger of b_0 or β, where $\beta=[C/D]^{1/4}$ with $C=\frac{2}{5}(\gamma_I\gamma_S\hbar)^2S(S+1)[\tau_e/(1+\omega_I^2\tau_e^2)]$.

In the diffusion-limited case [DL] $\beta>b_0$, and Eq. (5) becomes

$$\frac{1}{T_1}=\left[\frac{4\pi}{3}C\right]^{1/4}D^{3/4}, \tag{6}$$

while for the rapid diffusion case [RD] the following expression applies:

$$\frac{1}{T_1}=\frac{4\pi}{3}\frac{n_sC}{(\gamma_S\hbar S)^{3/2}}\left(\frac{\Delta\omega}{\omega_I}\right)^{3/4}\left(\frac{k_BT}{3a_0}\right)^{3/4}, \tag{7}$$

provided $\tau_e \ll T_2$. Crossover behavior from [DL] to [RD] relaxation may be expected with a decrease in temperature, and care must be exercised in applying the above expressions.

III. EXPERIMENTAL DETAILS

The samples were prepared from the melt at the University of Bath with original stoichiometry[2–4] $(R_2O_3)_x(X_2O_3)_{0.25-x}(P_2O_5)_{0.75}$, and x in the range 0.01 to 0.25 (nominally), for $R=Er^{3+}$, Nd^{3+}, Sm^{3+} and Gd^{3+}, and $X=Y^{3+}$ or La^{3+}.

^{31}P NMR measurements at 8.5 MHz (0.49 T) and 19.25 MHz (1.1 T) were made using a pulsed NMR spectrometer

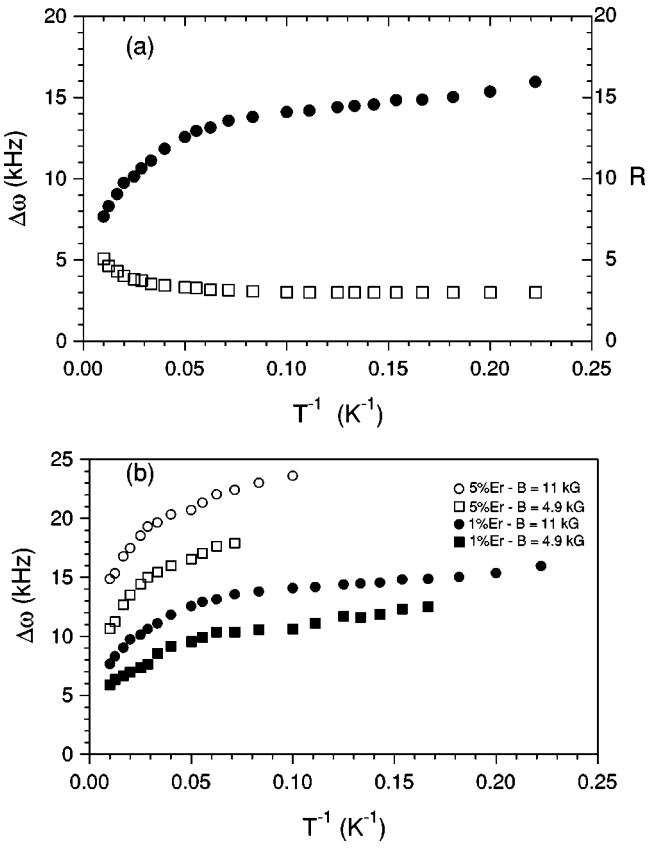

FIG. 1. (a) Inhomogeneously broadened nuclear resonance linewidth (dots) and moment ratios (squares) for a 1% Er REMG with $B=1.1$ T. (b) Inhomogeneously broadened nuclear resonance linewidths for 1% Er and 5% Er REMG with $B=0.49$ T and $B=1.1$ T.

and a Varian electromagnet. Data capture and processing were carried out using a Nicolet 430 oscilloscope interfaced to a desk top computer. Temperature control was achieved using a Janis helium cryostat and a Lakeshore DRC-93A temperature controller. A calibrated carbon glass resistor was used to measure the sample temperature.

Nuclear resonance line shapes have been characterized in terms of the moments of the resonance line determined from the Fourier transform frequency-domain NMR spin-echo wave forms for samples with large inhomogeneous broadening. A conventional three-pulse spin-echo method was used to measure T_1 whenever spin echoes could be observed. At lower temperatures some of the measurements were made using free induction decay signals.

IV. RESULTS AND DISCUSSION

A. ^{31}P line shapes

Nuclear resonance line shapes for the REMG have been characterized in terms of the moments of the resonance line, using $\Delta\omega=\langle M_2\rangle^{1/2}$, and the moment ratio, $R=\langle M_4\rangle/\langle M_2\rangle^2$. The NMR resonance line is inhomogeneously broadened due to coupling of the nuclear and paramagnetic ion moments. Figure 1(a) shows plots of the inhomogeneously broadened ^{31}P nuclear resonance linewidth and moment ratio R versus inverse temperature for a 1% Er REMG at $B=1.1$ T. The linewidth increases from approximately 7 to approximately 16 kHz with decreasing temperature, reaching a plateau at approximately 20 K. The ratio R is close to 3 at low temperatures, suggesting a characteristically Gaussian line shape.[8] There is appreciable inhomogeneous broadening of the line even at the highest temperatures at which measurements were made, as the NMR lines are approximately an order of magnitude larger than our crude estimate of the homogeneous linewidth ($\Delta\omega\simeq 1$ kHz). Following the onset of motional narrowing, R increases to around 5, implying a change in line shape toward the Lorentzian form. This behavior is typical of all the glasses studied. Figure 1(b) shows plots of linewidth versus inverse temperature for various Er REMG samples. For each sample, the linewidth increases while the signal amplitude, instead of following Curie law behavior, decreases with decreasing temperature, eventually becoming unobservably weak over a small temperature range. This is consistent with the ideas presented in Sec. II in terms of the overlap of exclusion regions. The signal-to-noise ratio increases with increasing resonance frequency so that, for a given sample, the temperature range over which the line can be observed is somewhat larger for a larger applied field.

It appears that the maximum observed linewidth depends on the magnetic ion concentration, the particular ion present and the magnetic field. In all cases, the NMR signal became immeasurably broad over a very small temperature range at low temperatures. The relatively low maximum observed linewidth ($\Delta\omega_{\max}<25$ kHz) and the different values found for $\Delta\omega_{\max}$ for different experiments strongly suggest that the abrupt loss of signal at low temperatures is not associated with limited spectrometer bandwidth. This loss of signal appears to be linked to the overlapping of diffusion barriers when two or more neighboring ions contribute to the linebroadening process for a majority of nuclear spins as discussed above. A discussion of the loss of signal and the mechanisms associated with this effect has been given elsewhere.[5]

The ^{31}P spin-spin relaxation time, T_2, determined from the spin-echo envelope, is 260 μs, which is a factor of 2 longer than our rough estimate obtained from structural information. For the Er^{3+}, Nd^{3+}, and Sm^{3+} ion-doped glasses, the electron correlation time approaches the nuclear T_2 value at temperatures in the vicinity of 5 K. For Gd^{3+}, the temperature at which τ_e becomes comparable to T_2 is approximately 50 K. When $\tau_e\lesssim T_2$, we expect the diffusion and exclusion barrier radii to reach their maximum values.

B. Relaxation times

Figure 2(a) shows plots of ^{31}P relaxation rates T_1^{-1} versus T^{-1} for the 1% Nd, 6% Nd and metaphosphate Nd REMG for $B=4.9$ kG. The peak in the relaxation rate for the 1% Nd data corresponds to $\omega_n\tau_e=1$. The temperature range over which measurements could be made on the 6% Nd and metaphosphate ($\sim$25%) Nd REMG before the line broadened dramatically, rendering the signal unobservable, was insufficient to observe the peak in T_1^{-1}. It is clear that the

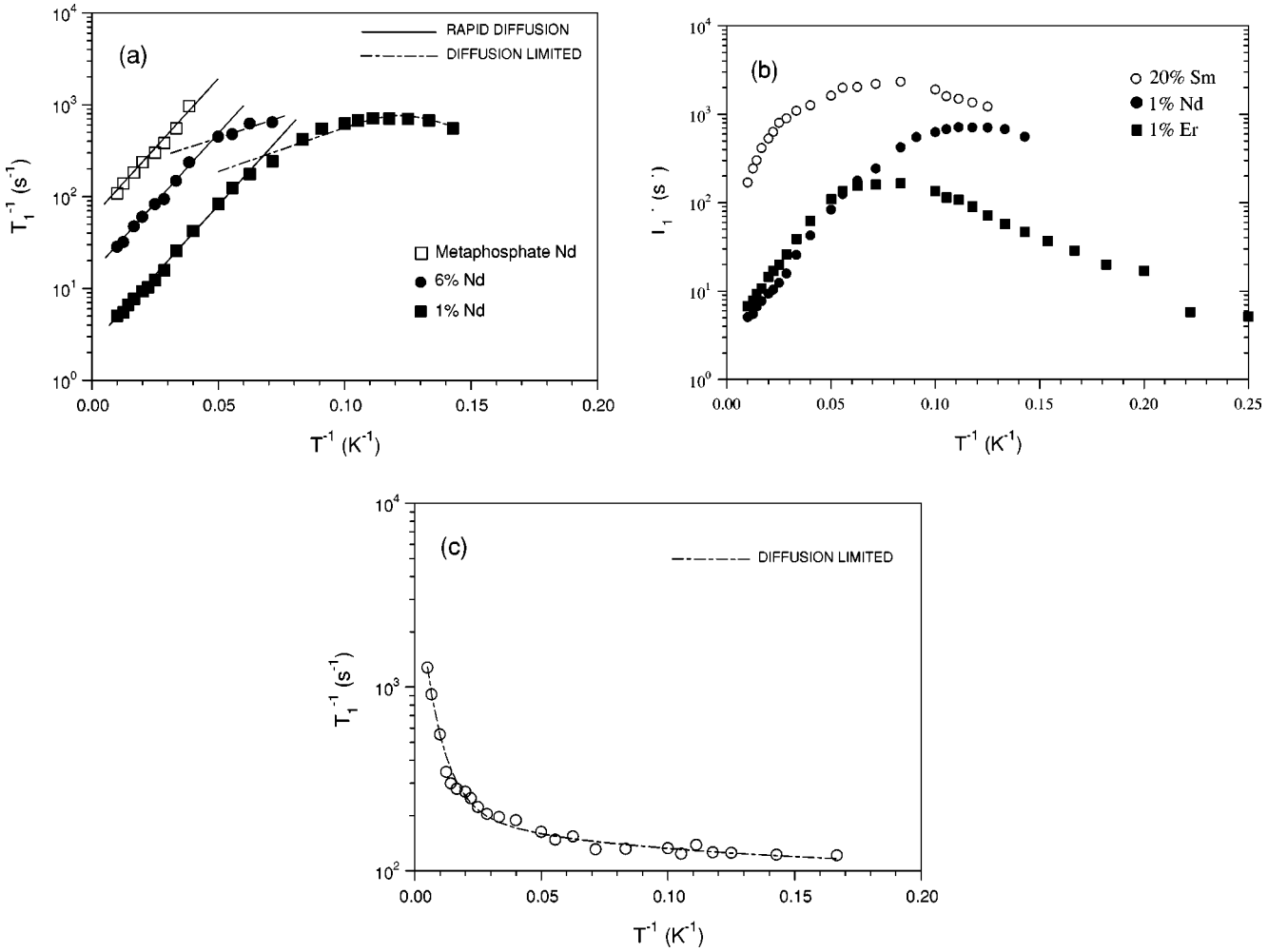

FIG. 2. (a) Plots of T_1^{-1} versus T^{-1} for 1% Nd, 6% Nd and metaphosphate Nd REMG. (b) Plots of T_1^{-1} versus T^{-1} for 1% Nd, 1% Er, and 20% Sm. (c) A plot of T_1^{-1} versus T^{-1} for 1% Gd REMG. The curves are the best fits to the experimental data of the [RD] and [DL] expressions.

nuclear relaxation rate is proportional to the magnetic ion concentration, but it appears that the metaphosphate Nd REMG contains a magnetic ion concentration somewhat lower than the nominal 25%. The data have been analyzed using Eqs. (6) [DL] and (7) [RD] to fit the low T and high T regions, respectively, as we justify below. The data for the metaphosphate concentration did not show any crossover from [DL] behavior to [RD] behavior before the signal disappeared. There is evidence to suggest that in the 6% Nd glass a crossover does occur, while the data for the 1% Nd glass are well described by a crossover from the [RD] expression above 20 K, to the [DL] expression at lower temperatures. This particular data set cannot be described consistently by a single [DL] expression. There are compelling physical reasons for expecting a crossover from [DL] behavior to [RD] behavior as the temperature decreases, since b_0 increases with decreasing temperature, and the condition $b_0 > \beta$ corresponding to Eq. (7) will be satisfied. The theoretical curves represent the best fits to the data of the [RD] and [DL] expressions applied in a consistent way.

If it is assumed that the RE ions occupy sites which approximate octahedral symmetry, it is justifiable to take over expressions derived for phonon-mediated relaxation processes in crystals and to examine how well they describe the present electron relaxation time results as a function of temperature. For ions with orbital angular momentum $L \neq 0$ crystal-field splitting of the ground state is important. In the case of Nd^{3+} the crystal field splits the $^4I_{9/2}$ free ion ground state into five Kramers doublets. In an applied magnetic field the ground-state degeneracy is lifted and the transitions between the two levels which are separated by an energy $\hbar\omega_e$ can occur. Similar energy levels are found for the other RE ions in crystal fields, with the exception of Gd^{3+} which has an ionic ground state $^8S_{7/2}$ $(L=0)$ and zero crystal-field splitting.

In crystals various phonon-mediated transition processes are important. These include the direct (single phonon), Raman (two phonon), and Orbach (two phonon) processes. Unlike the other two processes which involve transitions between the Zeeman split ground-state levels, Orbach processes involve excitation to a state at an energy Δ above the ground state. Typically, the crystal-field splitting $\Delta \gg \hbar\omega_e$. The resulting relaxation expression is[14–16]

TABLE I. Electronic relaxation parameters for magnetic rare-earth ions obtained from ^{31}P relaxation data. The quantities are defined in Eqs. (4) and (5).

	C_0 (s K^5)	$\Delta(K)$
Nd^{3+}	$2.7(3)\times10^{-7}$	88(5)
Er^{3+}	$1.6(3)\times10^{-7}$	102(5)
Sm^{3+}	$1.1(3)\times10^{-7}$	103(5)

$$\frac{1}{\tau e}=\frac{1}{C_D\Delta^2}T+\frac{1}{C_R\Delta^2}T^7+\frac{\Delta^3}{C_O}\frac{1}{\exp\left(\frac{\Delta}{k_BT}\right)-1}, \qquad (8)$$

where C_D, C_R, and C_O are relaxation constants for the direct, Raman and Orbach processes, respectively.

When $\Delta=0$, the relaxation expression involves different transition probabilities. The expression obtained for this case has the form[14]

$$\frac{1}{\tau e}=\frac{1}{C_D'}T+\frac{1}{C_R'}T^5, \qquad (9)$$

which exhibits a different temperature dependence for the Raman process than does Eq. (8). The quantities C_D' and C_R' are the relaxation constants for the direct and Raman processes, respectively, and are clearly different from the relaxation constants in Eq. (8).

Equations (8) and (9) assume a Debye phonon density of states. This is consistent with recent work,[17] including the soft potential model approach,[18] which suggests that vibrational modes in these systems are phononlike.

In Nd^{3+} REMG, the contributions to electronic relaxation from the Raman and direct processes are negligible, and the data were analyzed taking only the Orbach process into account for the temperature range covered in these experiments. All three Nd data sets were fitted using the same Orbach relaxation parameters. Both the line-shape data and the relaxation data provide no evidence that spin-spin interactions between the rare-earth ions are important over the temperature range covered in the present experiment.

Figure 2(b) shows plots of ^{31}P relaxation rates T_1^{-1} versus T^{-1} for the 1% Nd, 1% Er, and 20% Sm REMG. The nuclear relaxation rates for the Nd and Er REMG are similar at high temperatures. The peak in the Nd data occurs at a lower temperature than in the Er and Sm data. This suggests faster electronic relaxation in the Nd^{3+} ions, which results from a smaller crystal-field splitting than in the other REMG. Nuclear relaxation in the 20% Sm REMG is much faster than in the 1% Er and 1% Nd REMG because of the much higher dopant concentration.

For the 1% Gd REMG, electronic relaxation is much less efficient than in the other REMG due to the absence of the Orbach process. The condition $\omega_n\tau_e=1$ is not satisfied within the temperature range covered, and all the data are on the low-temperature side of the relaxation peak [Fig. 2(c)]. In Gd^{3+} REMG, the whole data set is well described by the [DL] expression. The direct relaxation process dominates relaxation below 20 K, while the Raman process is most important at higher temperatures. Electronic relaxation parameters for Nd^{3+}, Er^{3+}, and Sm^{3+} ions appear in Table I. For Gd^{3+} ions, the Orbach process is not operative, and direct and Raman processes determine the ionic relaxation time. We obtain $C_D'=8.1(2)\times10^{-2}$ (s K) and $C_R'=2.9(2)\times10^5$ (s K^5) for the Gd^{3+} REMG.

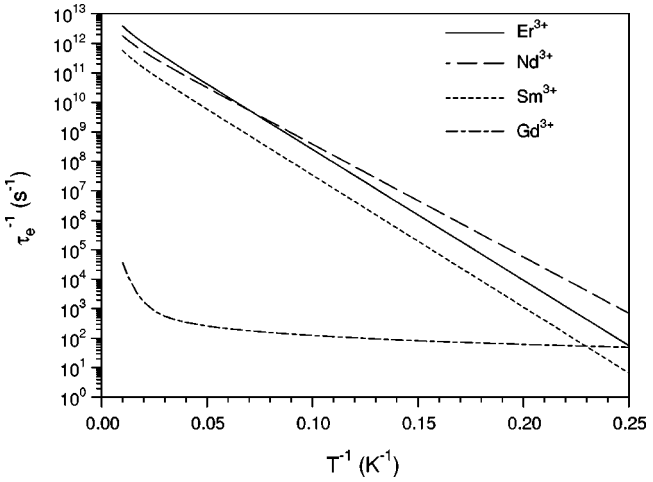

FIG. 3. Semilog plots of the electronic relaxation rate τ_e^{-1} extracted from nuclear relaxation data versus T^{-1} for the magnetic glasses studied.

The parameters listed in Table I, together with C_R' and C_D' for Gd^{3+}, have been used to generate logarithmic plots of the electronic relaxation rate τ_e^{-1} vs T^{-1} for the magnetic ions studied (Fig. 3). It can be seen that the relaxation rates for those ions in REMG with a crystal-field splitting, where the Orbach process can play a role, are much higher than for the Gd^{3+} REMG. As noted above, it is clear from Fig. 2(b) that the relaxation behavior of the 1% Nd and 1% Er glasses is very similar at higher temperatures. Figure 3 shows that a crossover in electron correlation times for these two systems occurs at around 15 K.

The quality of the fits of the relaxation expressions to the experimental data and the consistency of the fitting parameters between data sets provide strong support for the model as well as for the use of electronic relaxation expressions assuming a phonon density of states. Fractons[19] and ''excess'' modes[20] involving low-energy excitations do not appear to play a role in the electronic relaxation processes in these systems. In addition, the results obtained for the crystal-field energy gap Δ in the Nd-, Sm-, and Er-doped glasses seem to indicate that there is a surprisingly small distribution of crystal-field splittings. Further work is needed to confirm this.

V. CONCLUSION

It is clear from the results presented here that there is considerable inhomogeneous broadening of the ^{31}P resonance line in REMG. The line-shape changes in character from a Gaussian form to a Lorentzian form as the temperature increases. This is due to the decrease in the electron correlation time which leads to motional narrowing as T in-

creases. The abrupt loss of signal at low temperatures supports the model proposed for overlapping of nuclear spin diffusion and exclusion barriers in these materials.

Measurements of the ^{31}P spin-lattice relaxation time in metaphosphate glasses doped with rare-earth ions show strong evidence that the spin dynamics of these ions are governed by phonon mediated relaxation processes over a wide range of temperature. For Er-, Nd-, and Sm-doped glasses, the observed behavior with temperature is similar in all cases, with the spin correlation time being determined by a two-phonon Orbach process. The local environment of the ions is a distorted octahedron of oxygen atoms which give rise to crystal-field splittings. Estimates of the splitting are provided by the present work for the ions mentioned above, and the results indicate a small distribution of Δ values in the REMG. In the case of Gd-doped glasses, where no crystal-field splitting occurs, the paramagnetic ion correlation time is determined by direct and Raman processes. The approach we have established for determining details of paramagnetic ion behavior in these systems should be widely applicable to similar systems.

ACKNOWLEDGMENTS

Financial support from the National Research Foundation and the University of the Witwatersrand is gratefully acknowledged.

[1] G. Carini, G. D'Angelo, G. Tripodo, A. Fontana, F. Rossi, and G.A. Saunders, Europhys. Lett. **40**, 435 (1997).
[2] D.T. Bowron, R.J. Newport, B.D. Rainford, G.A. Saunders, and H.B. Senin, Phys. Rev. B **51**, 5739 (1995).
[3] D.T. Bowron, G. Bushnell-Wye, R.J. Newport, B.D. Rainford, and G.A. Saunders, J. Phys.: Condens. Matter **8**, 3337 (1996).
[4] D.T. Bowron, G.A. Saunders, R.J. Newport, B.D. Rainford, and H.B. Senin, Phys. Rev. B **53**, 5268 (1996).
[5] I.P. Goudemond, J.M. Keartland, M.J.R. Hoch, and G.A. Saunders, Hyperfine Interact. **120/121**, 545 (1999).
[6] I.P. Goudemond, J.M. Keartland, M.J.R. Hoch, and G.A. Saunders, Phys. Rev. B **56**, R8463 (1997).
[7] M. Goldman, *Spin Temperature and Nuclear Magnetic Resonance in Solids* (Clarendon, Oxford, 1970).
[8] A. Abragam, *The Principles of Nuclear Magnetism* (Oxford University Press, Oxford, 1961).
[9] A. Abragam and M. Goldman, *Nuclear Magnetism: Order and Disorder* (Clarendon, Oxford, 1982).
[10] H.E. Rorschach, Jr., Physica (Amsterdam) **30**, 38 (1964).
[11] G.R. Kutsishvili, Proc. Inst. Phys. Acad. Sci. Georgia (U.S.S.R.) **4**, 3 (1956).
[12] D. Tse and J. Lowe, Phys. Rev. **166**, 166 (1968).
[13] M.J. Duijvestijn, R.A. Wind, and J. Smidt, Physica B **138**, 147 (1986).
[14] A. Abragam and B. Bleaney, *Electron Paramagnetic Resonance of Transition Ions* (Clarendon, Oxford, 1970).
[15] C.B.P. Finn, R. Orbach, and W.P. Wolf, Proc. Phys. Soc. London **77**, 261 (1961).
[16] R. Orbach, Proc. R. Soc. London, Ser. A **264**, 485 (1961).
[17] G. Carini, G. D'Angelo, G. Tripodo, A. Fontana, A. Leonardi, G.A. Saunders, and A. Brodin, Phys. Rev. B **52**, 9342 (1995).
[18] V.G. Karpov, M.I. Klinger, and F.N. Igat'ev, Zh. Éksp. Teor. Fiz. **84**, 760 (1983) [Sov. Phys. JETP **57**, 439 (1983)].
[19] R. Orbach, Science **231**, 814 (1986).
[20] A. Fontana, F. Rocca, and M.P. Fontana, Phys. Rev. Lett. **58**, 503 (1987).